Planta (2017) 245:297–311
DOI 10.1007/s00425-016-2603-6

ORIGINAL ARTICLE

Changes in cuticular wax coverage and composition on developing Arabidopsis leaves are influenced by wax biosynthesis gene expression levels and trichome density

Lucas Busta[1] · Daniela Hegebarth[2] · Edward Kroc[3,4] · Reinhard Jetter[1,2]

Received: 19 July 2016 / Accepted: 29 September 2016 / Published online: 11 October 2016

Abstract

Main conclusion **Wax coverage on developing Arabidopsis leaf epidermis cells is constant and thus synchronized with cell expansion. Wax composition shifts from fatty acid to alkane dominance, mediated by *CER6* expression.**

Epidermal cells bear a wax-sealed cuticle to hinder transpirational water loss. The amount and composition of the cuticular wax mixture may change as organs develop, to optimize the cuticle for specific functions during growth. Here, morphometrics, wax chemical profiling, and gene expression measurements were integrated to study developing *Arabidopsis thaliana* leaves and, thus, further our understanding of cuticular wax ontogeny. Before 5 days of age, cells at the leaf tip ceased dividing and began to expand, while cells at the leaf base switched from cycling to expansion at day 13, generating a cell age gradient along the leaf. We used this spatial age distribution together with leaves of different ages to determine that, as leaves developed, their wax compositions shifted from C_{24}/C_{26} to C_{30}/C_{32} and from fatty acid to alkane constituents. These compositional changes paralleled an increase in the expression of the elongase enzyme CER6 but not of alkane pathway enzymes, suggesting that *CER6* transcriptional regulation is responsible for both chemical shifts. Leaves bore constant numbers of trichomes between 5 and 21 days of age and, thus, trichome density was higher on young leaves. During this time span, leaves of the trichome-less *gl1* mutant had constant wax coverage, while wild-type leaf coverage was initially high and then decreased, suggesting that high trichome density leads to greater apparent coverage on young leaves. Conversely, wax coverage on pavement cells remained constant over time, indicating that wax accumulation is synchronized with cell expansion throughout leaf development.

Keywords Arabidopsis mutant *gl1* · Epidermal cell development · Fatty acid elongase · Leaf development · Very-long-chain fatty acids · Wax analysis

Abbreviations

CER	ECERIFERUM
FAE	Fatty acid elongase
KCS	3-Ketoacyl-CoA synthase

Introduction

Plant organ development relies on the tightly controlled formation and expansion of various tissues based on limited resources of reduced carbon and nutrients. To protect

L. Busta and D. Hegebarth contributed equally to this work.

Electronic supplementary material The online version of this article (doi:10.1007/s00425-016-2603-6) contains supplementary material, which is available to authorized users.

✉ Reinhard Jetter
jetter@mail.ubc.ca

[1] Department of Chemistry, University of British Columbia, 2036 Main Mall, Vancouver, BC V6T 1Z1, Canada

[2] Department of Botany, University of British Columbia, 6270 University Boulevard, Vancouver, BC V6T 1Z4, Canada

[3] Department of Statistics, University of British Columbia, 3182 Earth Sciences Building, 2207 Main Mall, Vancouver, BC V6T 1Z4, Canada

[4] Department of Educational and Counselling Psychology, and Special Education, University of British Columbia, 2125 Main Mall, Vancouver, BC V6T 1Z4, Canada

precious new organs from adverse conditions, physical and chemical defenses are established early during development (Fraenkel 1959; Bennett and Wallsgrove 1994; Tian et al. 2012), and they must continuously expand to remain effective over the course of organ growth. Therefore, developing organs must continuously invest in both construction and protection of new structures (Coley et al. 1985; Zust et al. 2011; Bazzaz et al. 2016; Herms and Mattson 2016).

A balanced use of resources in leaf construction and protection is particularly important for epidermal cells because they form the leaf–environment interface. For example, the rapidly expanding epidermis of growing leaves must constantly protect the entire organ against physical damage, insect attack, and excessive water loss by transpiration. The plant epidermis is made up of pavement cells, guard cells, and trichomes. Pavement cells, the most abundant epidermal cell type on all organ surfaces, are the major protective surface barrier (Ramsay and Glover 2005). Guard cells, present on many organ surfaces in smaller numbers than pavement cells, are important for regulating gas exchange and for protecting the surface around stomata (Kearns and Assmann 1993). Finally, trichomes have a variety of roles including UV protection, heat insulation, transpiration control, and insect deterrence (Wagner et al. 2004). To gain insight into the various roles of epidermal cells, their development on leaves of various species including Arabidopsis has been studied in much detail (Glover 2000; Larkin et al. 2003; Guimil and Dunand 2007).

The three epidermal cell types, together comprising the organ–environment interface, are coated by a continuous lipophilic layer (Samuels et al. 2008; Yeats and Rose 2013). This extracellular membrane, the cuticle, consists of the polyester cutin and a mixture of hydrophobic wax compounds. The latter, typically present as a mixture of very-long-chain (VLC) fatty acids, primary alcohols, wax esters, aldehydes, and alkanes, constitutes the transpiration barrier (Schönherr 1976; Haas and Schönherr 1979; Isaacson et al. 2009). The amount of wax per surface area (coverage) and the composition of the wax mixture vary between tissues, organs, and species (Atkin and Hamilton 1950; Tulloch 1973; Salasoo 1983; Gülz et al. 1992; Viougeas et al. 1995; Jetter and Schäffer 2001; Richardson et al. 2005; Bringe et al. 2006; Kim et al. 2009; van Maarseveen et al. 2009), suggesting characteristic adaptations to optimize specific functions.

Cuticular wax ontogeny had been investigated in some species and, in most cases, had been found to be dynamic with respect to time. For example, changes in wax coverage and the composition of the cuticular wax mixture during development had been reported for leaves of *Kalanchoe daigremontiana* (van Maarseveen et al. 2009), *Prunus laurocerasus* (Jetter and Schäffer 2001), *Coffea arabica* (Stocker and Ashton 1975), *Malus domestica* (Bringe et al. 2006), *Sesamum indicum* (Kim et al. 2009), *Hordeum vulgare* (Richardson et al. 2005), *Triticum aestivum* (Tulloch 1973), *Hedera helix* (Viougeas et al. 1995), and *Fagus sylvatica* (Prasad and Gülz 1990) and fruits of *Prunus avium* (Peschel et al. 2007) and *Solanum lycopersicum* (Leide et al. 2007). Thus, the observed dynamics of cuticular wax suggest that coverages and compositions may not only be optimized for diverse functions between tissues, organs, and species, but also during discrete developmental stages.

To further increase our understanding of cuticular wax coverage, composition, and function on developing organs, integrated approaches combining organ morphometrics, wax chemical profiling, and gene expression analyses of a model species are required. Accordingly, cell expansion rates, wax composition, and expression levels of wax biosynthesis genes had been investigated in bolting stems of *Arabidopsis thaliana* (Suh et al. 2005), the species in which wax biosynthesis pathways are currently best characterized. It is well established that wax biosynthesis relies on plastid-derived fatty acyl-CoAs, which are converted by the fatty acid elongase (FAE) multi-enzyme complex to VLC acyl-CoAs with chain lengths between C_{22} and C_{38}. The chain length distribution of acyl-CoAs generated by the FAE is primarily determined by its 3-ketoacyl-CoA synthase (KCS) component enzymes (Millar and Kunst 1997) and associated proteins CER2 and CER26 (Haslam et al. 2015). The acyl-CoAs are then passed to either the acyl reduction pathway enzymes CER4 and WSD1 that generate primary alcohols and wax esters (Rowland et al. 2006; Li et al. 2008), or the alkane pathway enzymes CER3 and CER1 that produce aldehydes and alkanes, respectively (Bernard et al. 2012). Though fatty acids are major wax compounds on Arabidopsis leaves, their biosynthesis is not yet fully understood.

Interestingly, expanding Arabidopsis stem sections had been found to express many wax biosynthesis genes more highly than sections that had completed expansion, pointing to transcriptional regulation of wax biosynthesis (Suh et al. 2005). Nonetheless, neither wax coverage nor composition differed between the top, middle, and bottom sections of the stem, which had been sampled as proxies for organs of different age. However, Arabidopsis stems grow very rapidly, mainly by expanding in a very short zone near the top of the stem, rendering potential morphological, chemical, or genetic gradients within this zone only visible via analyses with very high spatial and temporal resolution.

In contrast to bolting inflorescence stems, Arabidopsis rosette leaves develop much more slowly and may, therefore, be good candidates for identifying developmental changes in wax coverage and/or composition that can be linked to cell expansion and gene expression. Arabidopsis

leaf waxes consist mainly of alkanes and primary alcohols, together with fatty acids and aldehydes (Jenks et al. 1995). An early study on the dynamics of Arabidopsis leaf waxes had found that whole rosettes from young plants have higher wax coverage, higher percentages of fatty acids, and longer alcohols than whole rosettes from older plants (Jenks et al. 1996). Here, we sought to improve our understanding of the relationships between leaf development and wax biosynthesis by first corroborating previous wax profiling results with higher temporal resolution using leaves from only one nodal position and then integrating these measurements with epidermal cell development and gene expression data. Leaves of wild-type and trichomeless (*gl1*) Arabidopsis plants were harvested every 4 days during development, and investigated using light and confocal microscopy, gas chromatography (GC) with flame ionization detection (FID) or coupled with mass spectrometry (MS), and quantitative RT-PCR.

Materials and methods

Plant material, growth conditions, and leaf harvesting

Arabidopsis thaliana wild-type (Col-0) and *gl1* (SALK_039478C) seeds were germinated on agar plates and then transferred to and grown in soil as described previously (Lai et al. 2007). Preliminary tests had shown that under our conditions leaves on nodes one to seven grew to variable, relatively small sizes, while leaves on nodes eight and higher all grew to approximately the same full size. Therefore, eighth rosette leaves were chosen for monitoring, and the lengths of eighth leaf blades and petioles were determined daily using a ruler.

Leaf morphological analysis

Eighth leaves were harvested every 2 days between 5 and 21 days of age for morphometrics. Five leaves were segmented (Fig. S1), then each segment was stained with propidium iodide (100 mg/ml; Sigma, Oakville, ON, Canada) to visualize cell outlines, and four images of the abaxial side of each segment were captured with a confocal laser-scanning microscope (Radiance 2000; Bio-Rad, Hercules, CA, USA; excitation 568 nm, emission 580–600 nm). Images were processed with ImageJ to obtain the total area and number of pavement and guard cells on each segment. The mean number and size of cells on each leaf were determined by averaging across segments. The adaxial sides of five more leaves were photographed under a dissecting light microscope, and the number of trichomes was counted and averaged.

Wax sample preparation and gas chromatography (GC) analysis

Eighth leaves were harvested every 4 days between 5 and 21 days of age by cutting between blade and petiole. Leaf blades with a sum surface area of at least 10 cm^2 were dipped in two volumes of chloroform for 30 s each, then the volumes were combined and the solvent evaporated under nitrogen to produce a single wax sample. Five independent samples were prepared at each time point. Wax samples were analyzed with GC–MS and GC–FID as described previously (Buschhaus and Jetter 2012). To detect meaningful trends over time, R (R Core Team 2015) was used to conduct permutation tests on the ordinary least-squares slopes of the data from *gl1* mutant and wild-type leaves. A total of 42 tests were performed using the *gl1* mutant data (see Fig. 3): one for each compound class (seven tests), one for the relative abundance of each homolog within the total wax mixture (26 tests), and one for the relative abundance of the sum total of compounds derived from each precursor chain length (nine tests). The same tests were also performed on the data from wild-type leaves (see Fig. 4). Example R code used to conduct this analysis appears in Appendix S1.

For leaf tip and base analyses, 30 eighth leaves at 13 days of age were harvested, cut into thirds, and the 30 tip sections and 30 base sections were divided into four independent sets each. Prior to extraction, each independent set of leaves was photographed alongside a ruler, and ImageJ was used to count leaf pixels to determine the surface areas extracted. Waxes from each independent set of leaves were then extracted and analyzed in the same way as the whole-leaf wax samples. A total of 29 permutation tests on the mean difference between the relative abundance of each homolog in each compound class of the base and tip samples were performed to detect significant effects (see Fig. 6). Example R code used to conduct this analysis appears in Appendix S1.

RNA extraction and gene expression analysis by quantitative RT-PCR

For gene expression analysis, eighth leaves were harvested every 4 days between 5 and 21 days of age and immediately frozen in liquid N_2. An average amount of 50 mg fresh plant material was homogenized with Zirconia beads (2 nm diameter, BioSpec Products, Bartlesville, OK, USA) at 4 °C using a Precellys-24 homogenizer (Bertin, Rockville, MD, USA) (2000*g*, 2 × 25 s). Total RNA was extracted using a PureLink RNA mini kit (Invitrogen, Carlsbad, CA, USA) as described in the manufacturer's protocol. On-column DNA digestions were performed using PureLink DNase Set (Invitrogen) following the manufacturer's protocol. The integrity of extracted RNA and absence of genomic DNA

was confirmed by agarose gel electrophoresis (2 %), and concentrations and purity were determined by acquiring UV spectra and calculating 260/280 nm and 260/230 nm ratios using a NanoDrop 8000 Spectrophotometer (Thermo Fisher Scientific, Waltham, MA, USA). Samples with a ratio between 1.7 and 2.2 were selected as templates for qRT-PCR. For first-strand cDNA synthesis, 5 µg total RNA and Oligo(dT)$_{20}$ primers (Invitrogen) were used together with SuperScript Reverse Trancriptase II (Invitrogen) following the manufacturer's protocol, and the resulting cDNA samples were stored at −20 °C.

The expression level of wax biosynthesis genes was measured by quantitative RT-PCR using iQ SYBR Green Supermix (Bio-Rad) following the manufacturer's procedure and using gene-specific primers (Table S1). Hard-shell 96-well PCR plates with thin walls were used (Bio-Rad) with the CFX Connect Real-Time PCR Detection System (Bio-Rad) under the following PCR conditions: one cycle at 95 °C for 3 min, followed by 40 cycles at 95 °C for 15 s, and at 60 °C for 30 s. A total amount of 50 ng cDNA was used in a 10-µl reaction volume. Each sample was run in triplicate alongside a no-template control, and five to seven independent measurements of each gene's expression level were made at each time point. Melting curves were acquired after each run to verify primer specificity. The primer efficiency was tested for each primer pair (between 93 and 108 %, Table S2) and used for normalization. CFX Connect Real-Time PCR Detection System software (Bio-Rad) was used for data acquisition, and data were analyzed by adjusting the threshold cycles. Relative expression (Table S3) was calculated using the Pfaffl method (Pfaffl 2001). To account for variation in the amount of tissue harvested, the expression levels of target genes had to be normalized. Preliminary experiments showed that, of the four reference genes *Actin2*, *GAPDH*, *UBQ10*, and *UBC21*, the latter exhibited the most stable expression over all time points (data not shown), and it was, therefore, used to normalize expression levels of target genes.

Just as for the chemical data, permutation tests were conducted on the least-squares slopes of the expression profiles of the 12 genes to detect significant changes over time. To determine which effects remained robust to tempering of possible inflation of gene expression levels at day 5, a sensitivity analysis of these effects was performed. The output of these statistical procedures is summarized in Fig. 7, while R code and full details of the statistical analysis appear in Appendix S1.

Adjustment for multiple comparisons

To control possible inflation of the rate of Type I error due to the many statistical comparisons being made, the Benjamini–Hochberg method was used so that the study-wide expected proportion of falsely rejected null hypotheses was no more than 1 % (Benjamini and Hochberg 1995). All effects found statistically significant according to this procedure were flagged with an asterisk.

Results

The goal of this study was to link changes in cuticular wax coverage and composition on growing Arabidopsis leaves with epidermal cell development and potential changes in the expression of underlying wax biosynthesis genes. First, eighth leaf blade and epidermal cell surface areas were determined, together with the numbers of epidermal cells present. Wax coverage and composition on leaves without and with trichome cells were measured every 4 days during growth, and pavement cell size and wax composition on discrete leaf sections were determined. Finally, the expression levels of wax biosynthesis genes were measured over the course of leaf development.

Morphological changes on developing leaves

Leaf surface areas and the numbers of epidermal cells were measured as a function of leaf age. Under the growth conditions used here, leaf blades expanded steadily from 10 mm^2 at day 5 to 138 mm^2 at day 21 (Fig. 1a), after which they did not change (Table S4). The average surface area of (abaxial) pavement cells increased from ca. 490 to 3910 µm^2 between days 5 and 21 (Fig. 1a), and, thus, pavement cell expansion accounted for the majority of macroscopic leaf growth. However, leaf expansion was also partially due to pavement cell division, which led the number of pavement cells to increase from ca. 20,500 per blade at day 5 to ca. 29,100 by day 13 and remain roughly constant thereafter (Fig. 1b). Concomitantly, the number of (abaxial) guard cell pairs increased from day 5 (ca. 6700 per blade) to day 13 (10,100) and then also stayed constant (Fig. 1b). Based on numerous literature reports on Arabidopsis leaf epidermis development (Iwakawa et al. 2007; Chen et al. 2013), it can be assumed that the average sizes of guard cells and pavement cells were at all times similar on the adaxial and abaxial sides of the leaves studied here. The number of (adaxial) trichomes, ca. 75, was constant throughout eighth leaf development, resulting in relatively high trichome densities on younger leaves and a steady decrease in trichome density as the leaf expanded (Fig. 1b).

Wax development on growing eighth rosette leaves of the trichome-less Arabidopsis mutant *gl1*

To delineate effects arising from shifts in the relative abundance of trichome cells over time, the waxes from

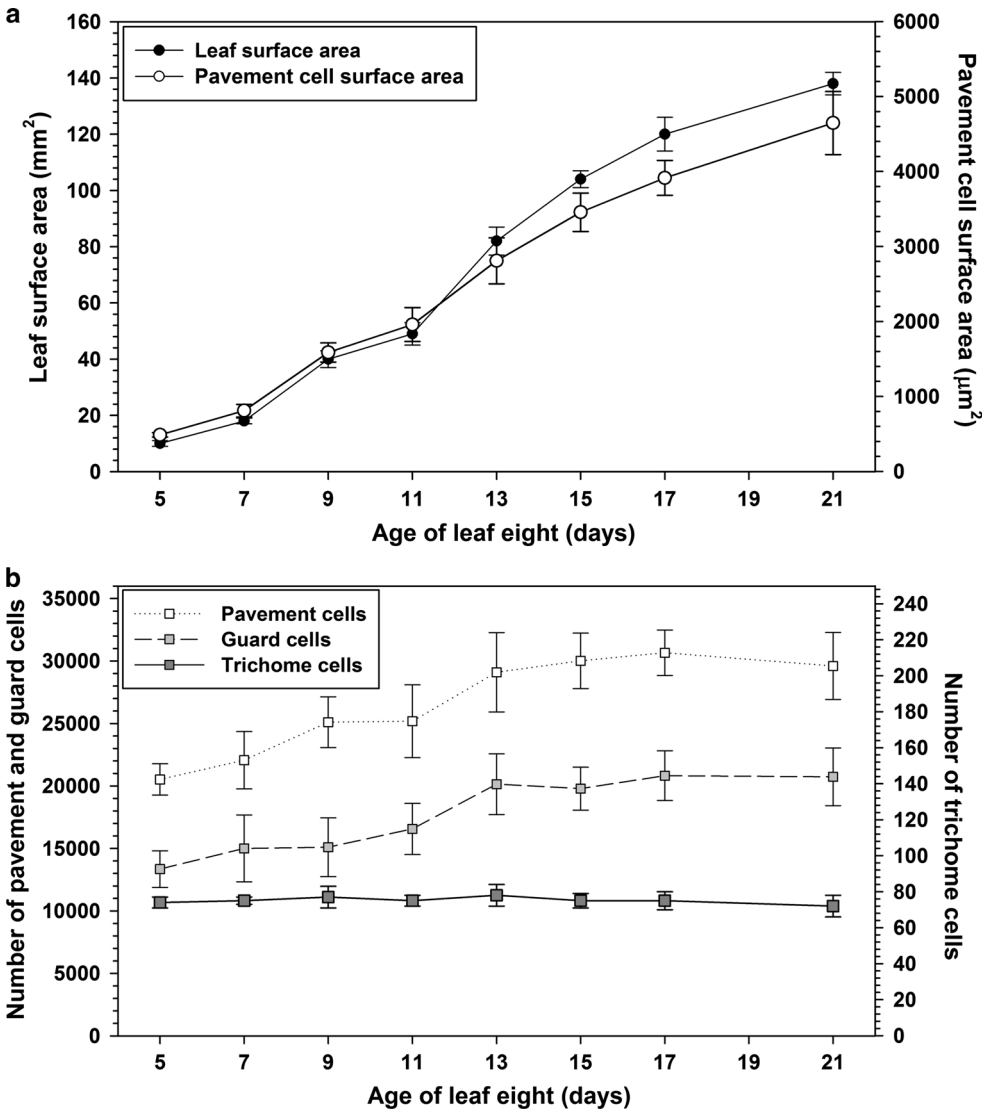

Fig. 1 Surface area and epidermal cell numbers on developing wild-type Arabidopsis eighth rosette leaves. **a** Leaf surface area (*black circles*, left *y*-axis) and abaxial pavement cell surface area (*white circles*, right *y*-axis) measured between 5 and 21 days of leaf age. **b** Number of abaxial pavement cells (*white squares*, left *y*-axis), abaxial guard cells (*light grey squares*, left *y*-axis), and adaxial trichome cells (*dark grey squares*, right *y*-axis) measured between 5 and 21 days of leaf age. *Point positions* and *error bars* indicate the mean and standard deviation of five independent measurements, respectively

developing leaves of both the trichome-less mutant *gl1* and wild-type plants were extracted every 4 days during growth and analyzed with GC–MS and GC–FID. Five-day-old *gl1* leaves were covered with 0.62 ± 0.05 µg/cm^2 extractable wax (Fig. 2) made up of fatty acids (34 % of the overall wax mixture), alkanes (26 %), branched alcohols (13 %), *n*-alcohols (7 %), aldehydes (2 %), alkenes (2 %), and 16 % unidentified compounds (Fig. 3a; Table S5). At 21 days of age, *gl1* leaves bore 0.64 ± 0.04 µg/cm^2 wax, which was composed of alkanes (42 %), fatty acids (19 %), branched alcohols (11 %), *n*-alcohols (7 %), aldehydes (5 %), and alkenes (2 %), leaving 14 % unidentified. Thus, wax coverage remained constant over the course of *gl1* leaf development, and after day 5, the composition of the mixture gradually shifted, becoming significantly less fatty acid- and more alkane-dominated.

Each of the chemical classes was present as a homologous series spanning chain length ranges typical of cuticular wax compounds. Fatty acids were present with even carbon numbers between C_{22} and C_{32}, within which the C_{24} and C_{26} homologs were the most prominent (Fig. 3b). The *n*-alcohols also had predominantly even carbon numbers, but ranged from C_{26} to C_{34} with an approximately normal distribution. Three branched-chain alcohols with total carbon numbers C_{30}, C_{32}, and C_{34} were identified, with the C_{32} homolog being the most abundant. Four unbranched aldehydes with even carbon numbers from C_{28} to C_{34} were detected in roughly equal amounts. *n*-Alkanes were found with odd carbon numbers ranging from C_{27} to C_{37}, the C_{29}, C_{31}, and C_{33} homologs being the most abundant. Finally, C_{35} and C_{37} *n*-alkenes were present in roughly equal amounts.

Chain length shifts were observed during *gl1* leaf development, and were most pronounced within the fatty acid and alkane series. From day 5 to day 21, the relative abundance of C_{24} fatty acid decreased steadily from 13 to

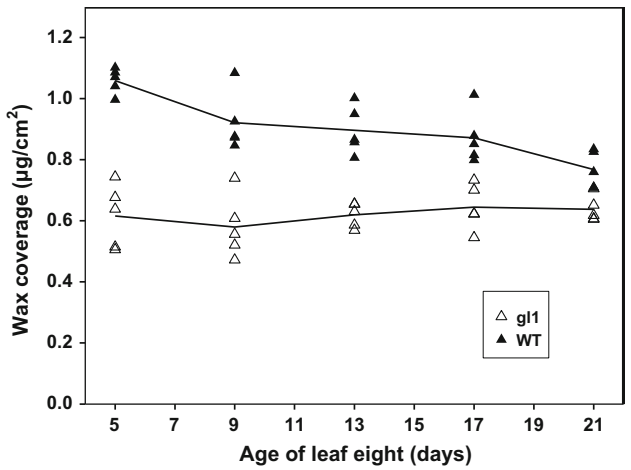

Fig. 2 Wax coverage on developing Arabidopsis *gl1* and wild-type eighth rosette leaves. The total amount of wax from *gl1* and wild-type is expressed as wax mass (µg) per surface area extracted (cm^2). Eighth rosette leaves were harvested every 4 days from 5 to 21 days of leaf age, and their total wax coverages were measured with GC–FID. *Lines* connect the mean of the five independent measurements

3 % of the total wax mixture (Fig. 3b). Simultaneously, relative amounts of C_{29} and C_{31} alkanes increased steadily from ca. 7 to 18 % and 9 to 18 %, respectively, while the relative abundance of C_{33} alkane decreased from 11 to 3 %. Thus, a significant, combined shift from acid- to alkane-dominance and from C_{24} to C_{29} and C_{31} compounds was observed over the course of development on *gl1* leaves.

Finally, the overall chain length profiles across all compound classes within the wax mixture on developing *gl1* leaves were calculated. For this, the relative amounts of all compounds formed by modification of the same acyl-CoA precursor were added together, e.g. C_{30} acid, C_{30} alcohols, C_{30} aldehyde, and C_{29} alkane. At 5 days of age, *gl1* leaf wax was made up of ca. 22 % each C_{26} and C_{32} compounds, and ca. 16 % each C_{24}, C_{30}, and C_{34} compounds (Fig. 3c). At 21 days of age, the mixture contained ca. 45 % C_{32} compounds, 30 % C_{30} compounds, and 26 % C_{26} compounds, together with smaller amounts of C_{24} and C_{34} compounds. Relatively minor quantities of compounds

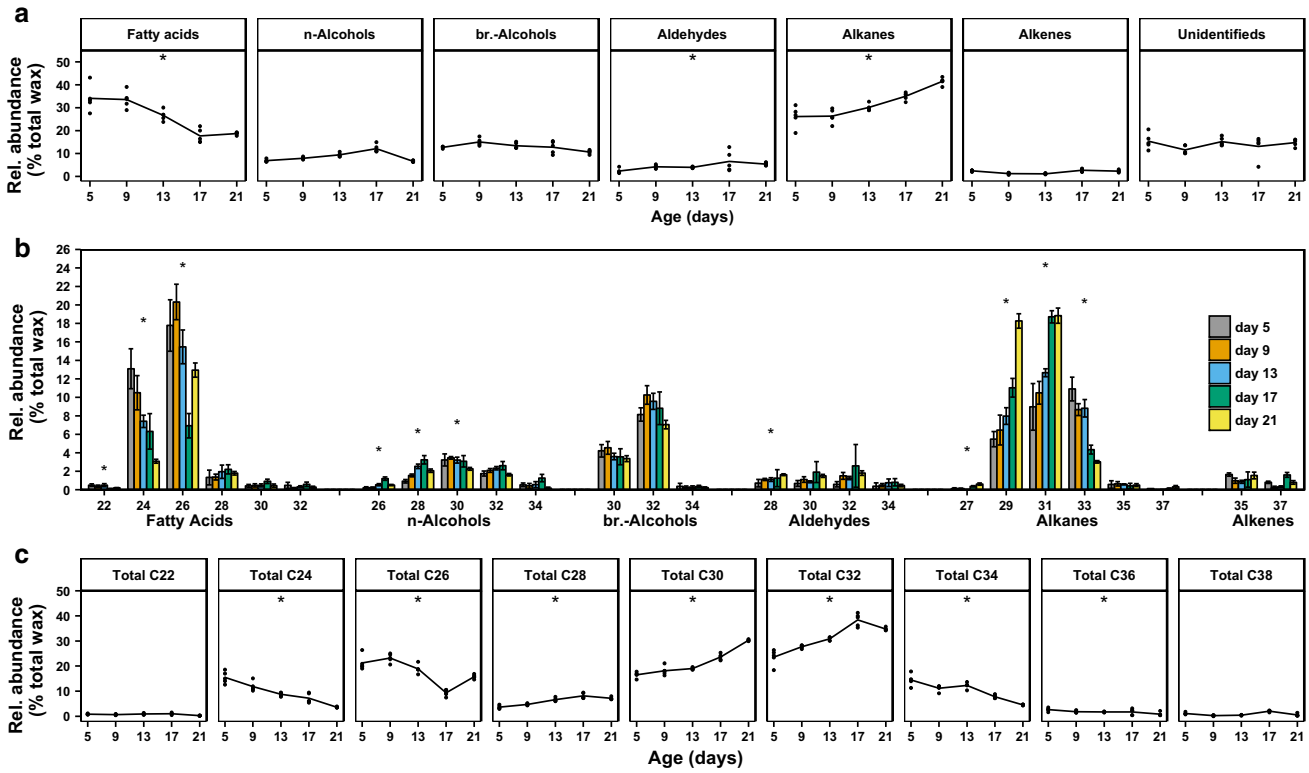

Fig. 3 Wax composition on developing Arabidopsis *gl1* mutant eighth rosette leaves. **a** Relative abundance of each compound class as a function of leaf age. **b** Relative abundance of each wax compound as a function of leaf age. Labels on the *x*-axis indicate the carbon number and class of each identified compound. **c** Relative abundance of each chain length as a function of leaf age. Odd-numbered homologs of alkanes and alkenes are derived from even-numbered precursors with one carbon more, and these compounds are, therefore, grouped with compounds derived from respective precursors with even total carbon numbers. *Bar heights* and *error bars* indicate the mean and standard deviation of five independent measurements, respectively. *Lines* connect the means of the five independent measurements made at each time point. *Asterisks* indicate significant time-dependent changes derived from a permutation test of the ordinary least-squares linear fit after study-wide adjustment for multiple comparisons

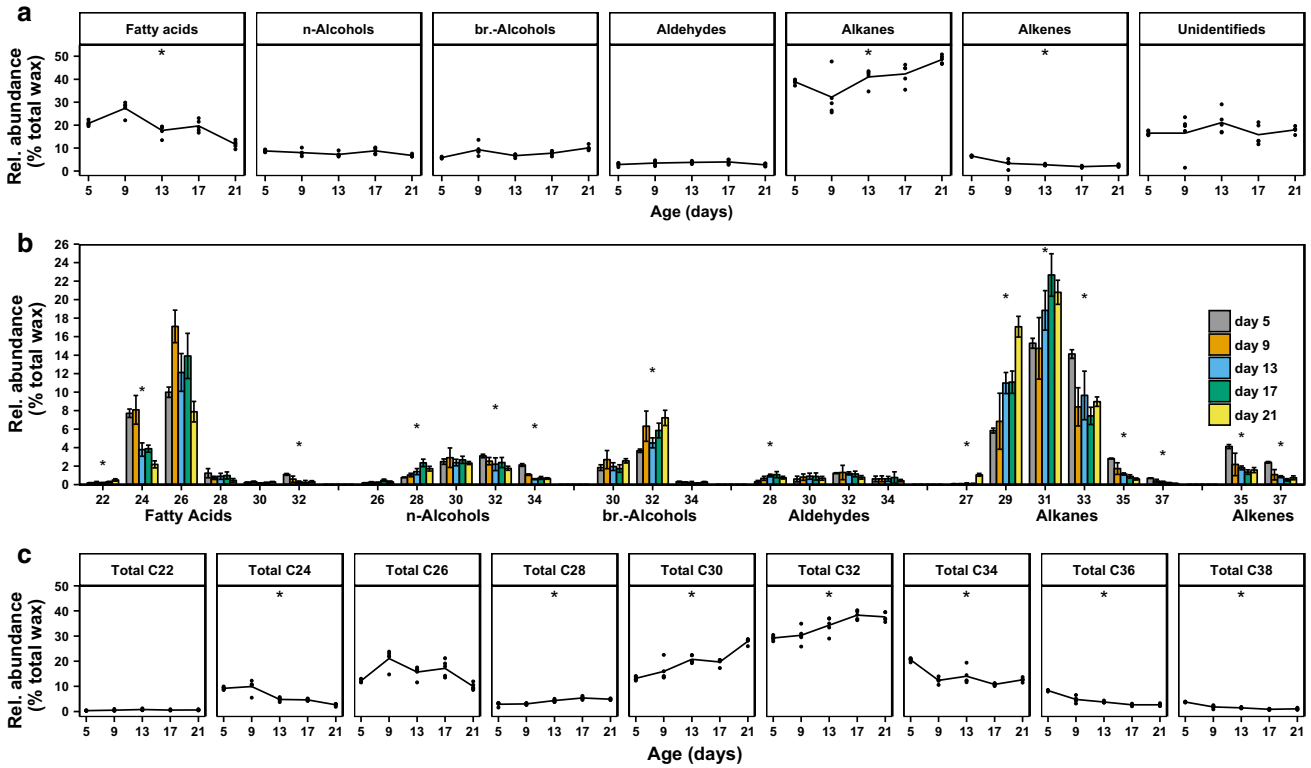

Fig. 4 Wax composition on developing Arabidopsis wild-type eighth rosette leaves. **a** Relative abundance of each compound class as a function of leaf age. **b** Relative abundance of each homolog within compound classes as a function of leaf age. Labels on the *x*-axis indicate the carbon number and class of each identified compound. **c** Relative abundance of each chain length as a function of leaf age. Odd-numbered homologs of alkanes and alkenes are derived from even-numbered precursors with one carbon more, and these compounds are, therefore, grouped with compounds derived from respective precursors with even total carbon numbers. *Lines* connect the means of the five independent measurements made at each time point. *Asterisks* indicate significant time-dependent changes derived from a permutation test of the ordinary least-squares linear fit after study-wide adjustment for multiple comparisons

with chain lengths C_{22}, C_{28}, C_{36}, and C_{38} were present throughout development. Overall, the most pronounced changes over time were observed as increases in the relative abundance of C_{32} and C_{30} compounds and decreases in the relative abundance of C_{24}, C_{26}, and C_{34} compounds.

Wax development on growing eighth rosette leaves of wild-type Arabidopsis

The cuticular wax of wild-type eighth rosette leaves was harvested and analyzed in the same way and at the same points during development as described for *gl1*. Coverage on wild-type leaves decreased significantly between 5 days of age (1.06 ± 0.02 µg/cm^2) and 21 days of age (0.86 ± 0.06 µg/cm^2, Fig. 2; Table S6).

The wax on 5-day-old wild-type eighth leaves contained alkanes (39 %), fatty acids (21 %), *n*-alcohols (9 %), branched alcohols (6 %), alkenes (7 %), and aldehydes (3 %), leaving 15 % of the wax unidentified. Alkanes were the most prominent compound class throughout the development of wild-type leaves, increasing significantly from 39 to 49 % of the total wax mixture between days 5 and 21 (Fig. 4a). Over the same time interval, the relative abundance of fatty acids and alkenes decreased significantly from 20 to 12 % and from 7 to 2 %, respectively, while other compound classes exhibited relatively little fluctuation.

Wild-type leaf wax contained homologous series of fatty acids (C_{22}–C_{32}), *n*-alcohols (C_{26}–C_{34}), branched alcohols (C_{30}–C_{34}), and aldehydes (C_{28}–C_{34}), all with predominantly even carbon numbers, as well as alkanes (C_{27}–C_{37}) and alkenes (C_{35}–C_{37}) with predominantly odd carbon numbers (Fig. 4b). Overall, the same compounds were identified in the leaf waxes of wild type and the *gl1* mutant. Homolog distributions within these chain length ranges were also similar on both lines. Over time, the relative abundance of C_{24} fatty acid decreased significantly from ca. 8 to 2 % in wild-type wax, while C_{29} and C_{31} alkanes increased significantly from 5 to 17 % and from 15 to 20 %, respectively. In contrast, the relative abundances of the longer alkanes (C_{33}, C_{35}, and C_{37}) as well as C_{35} and C_{37} alkenes decreased significantly over time.

In terms of constituent chain lengths, wild-type leaf wax was made up of 29 % C_{32} compounds, ca. 20 % C_{34}

compounds, 13 % each C_{26} and C_{30} compounds, ca. 9 % each C_{24} and C_{36} compounds, and ca. 4 % C_{38} compounds at day 5 (Fig. 4c). At 21 days of age, the mixture consisted of 38 % C_{32}, 28 % C_{30}, 13 % C_{26}, 11 % C_{34} compounds, ca. 2 % each C_{24} and C_{36} compounds, and 1 % C_{38} compounds. Thus, the relative abundance of C_{30} and C_{32} compounds increased significantly over time, while that of C_{24}, C_{34}, C_{36}, and C_{38} compounds decreased significantly. Throughout development, C_{22} compounds contributed relatively minor amounts to the total wax mixture.

Regional distribution of wax on Arabidopsis leaves

To test whether differences in wax composition also existed between discrete leaf regions potentially differing in average cell age, leaves were sectioned (Fig. S1), and the size distribution of pavement cells on each section was investigated. Five-day-old leaves exhibited a pavement cell size gradient along their longitudinal axes from 300 ± 50 μm^2 at the base of the blade to 900 ± 200 μm^2 at the tip (Fig. 5; Table S7). A larger size difference was observed on leaves at day 9, where pavement cells varied in size from 1000 μm^2 at the base to 3000 μm^2 at the tip. Similar gradients were observed on leaves at days 13 and 17. In contrast, at day 21, pavement cells along the entire blade were similar in size, ca. 5000 ± 1000 μm^2. Overall, the pavement cell size distributions indicated that pavement cells at the leaf tip initiated and completed expansion before those at the leaf base. At 13 days of age, leaves exhibited the largest difference in pavement cell size and age between leaf base and tip, with cells at the base most similar to those found on young leaves and cells at the tip most similar to those found on mature leaves.

To correlate pavement cell size and age with wax composition, 13-day-old leaves were cut into three equal-sized pieces, and the wax compositions of the base and tip segments were determined as described above for whole-leaf wax analysis. The identity and span of the classes of homologous compounds identified on both the leaf bases and tips were identical, containing fatty acids (C_{22}–C_{34}), *n*-alcohols (C_{24}–C_{34}), branched alcohols (C_{30}–C_{34}), aldehydes (C_{26}–C_{34}), alkanes (C_{27}–C_{37}), and alkenes (C_{35}–C_{37}), but the relative abundance of some of these compounds differed between the leaf tips and bases. In particular, C_{24} and C_{26} acids made up 5 and 14 % of the total wax on leaf bases, respectively, while on the tips they represented only 2 and 8 % (Fig. 6). Furthermore, leaf bases were covered with 9 and 13 % C_{29} and C_{31} alkanes, respectively, while these compounds comprised 17 and 19 % of the wax on leaf tips. The relative abundances of all other compounds were similar on leaf tips and bases.

Expression of wax biosynthesis genes during leaf development

To assess possible contributions of wax biosynthesis gene expression to fluctuations in wax production levels, transcript levels were monitored at the same time points used for wax sampling. Based on their function, the investigated genes were grouped as coding for (1) condensing enzymes of elongation complexes (KCSs), (2) proteins associated with the elongation complex(es), and (3) head-group-modifying enzymes.

Of the 21 *KCS* genes encoding condensing enzymes in Arabidopsis, five were selected for the current study based on previous reports showing their involvement in wax

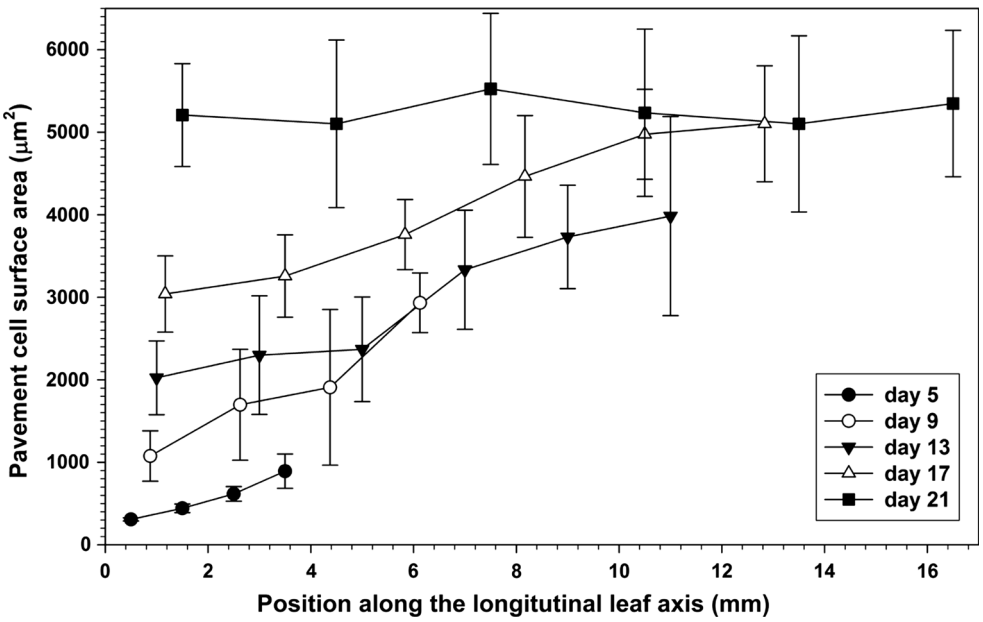

Fig. 5 Pavement cell size on segments of developing Arabidopsis wild-type eighth rosette leaves. Pavement cell surface areas (μm^2) are plotted as a function of their position along the longitudinal axis of the leaf (mm, measured from the leaf blade base) for leaves between 5 and 21 days of age. *Point positions* and *error bars* indicate the mean and standard deviation of five independent measurements, respectively

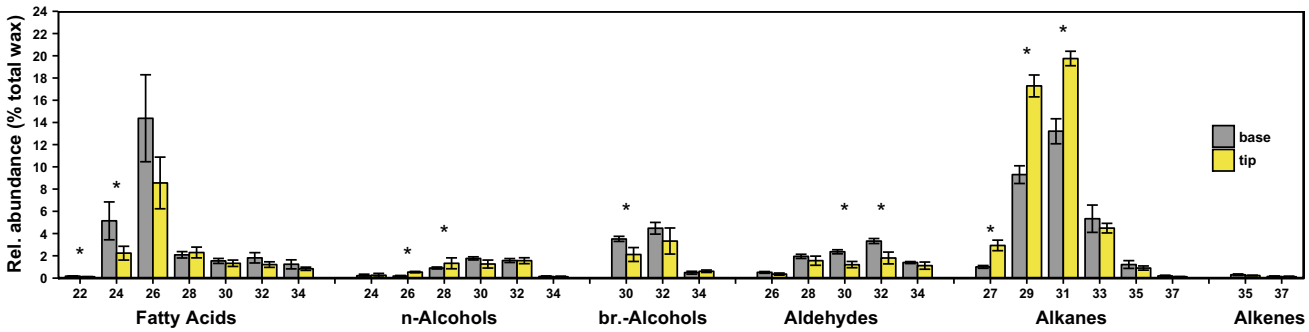

Fig. 6 Wax composition on the base and tip sections of wild-type Arabidopsis eighth rosette leaves at 13 days of age. The relative abundance of each homolog in each compound class is plotted as a percent of the total amount of extracted wax. Labels on the *x*-axis indicate the carbon number and class of each identified compound. Leaf base and tip samples were prepared by selecting eighth leaves at 13 days of age, cutting them into three equal segments, and independently extracting the base and tip segments. *Bar heights* and *error bars* indicate the mean and standard deviation of five independent measurements, respectively. *Asterisks* indicate significant mean differences between base and tip derived from a permutation test after study-wide adjustment for multiple comparisons

formation (Jenks et al. 1995; Fiebig et al. 2000; Hooker et al. 2002; Todd et al. 1999; Trenkamp et al. 2004), or based on publicly available in silico data (http://bar.utoronto.ca/eplant/) suggesting differential gene expression during leaf development or between epidermal cell types (Jakoby et al. 2008; Marks et al., 2009). Among the five *KCS* genes, *CER6* and *KCS8* were expressed at much higher levels than *KCS1*, *KCS5*, and *KCS16* (Fig. 7a). Over the course of leaf development, *KCS1* and *CER6* expression increased significantly, expression of *KCS8* decreased significantly, and that of *KCS5* and *KCS16* exhibited a slight decrease between days 5 and 13.

All the genes coding for other proteins associated with elongation, *CER10*, *CER8*, *CER2* and *CER26,* were expressed at relatively high and constant levels throughout leaf development (Fig. 7b), excepting the slightly higher expression of *CER10* and *CER8* at day 5. Among the head-group-modifying enzymes, *CER3* and *CER1* were expressed at intermediate levels and *CER4* at very low levels (Fig. 7c). Expression of *CER3* and *CER1* varied relatively little over the course of leaf development, excepting higher expression of *CER1* at day 5, while *CER4* expression increased slightly but significantly throughout development.

Discussion

Overall, our morphometric results first established that trichome density decreased steadily during leaf development, that leaf tip expansion preceded leaf base expansion, and that gradients in pavement cell maturity and size between leaf tips and bases were maximized around 13 days of leaf age. Wax coverage on wild type decreased significantly with expansion, while *gl1* had constant, lower coverage. An age-dependent shift from C_{24}/C_{26} to C_{30}/C_{32} compounds was accompanied by a relative decrease in fatty acid abundance and an increase in alkane abundance on both plant lines. Wild-type leaves also exhibited a simultaneous decrease in the relative abundance of C_{35+} compounds. qRT-PCR analyses revealed that head-group-modifying enzymes were expressed at fairly constant, albeit different levels. An increase in the expression of *KCS1* and *CER6* was accompanied by a decrease in that of *KCS5* and *KCS16*, whereas non-*KCS* elongation genes were expressed at roughly constant levels throughout leaf development. These findings can now be integrated to discuss wax dynamics in the context of pavement cell age, leaf expansion, and epidermal cell composition.

Pavement cell age effects on wax composition

We monitored Arabidopsis leaf morphology to give context to our wax composition and gene expression data. The data acquired here spanned leaf development from an early stage, defined by the onset of pavement cell expansion, to a late stage when pavement cell expansion was largely complete. This occurred after 21 days of growth, similar to previous observations of Arabidopsis leaf six (Granier et al. 2002). Like other studies on growing leaves from Arabidopsis and other species (Sylvester et al. 1990; Donnelly et al. 1999; Nath et al. 2003; Byrne 2005; Efroni et al. 2010), we found that pavement cells near the leaf tip began to expand at a time when many cells near the base were still dividing, and that tip cells finished expansion long before base cells. Thus, the position of a pavement cell along the leaf axis is related to cell age, with the youngest cells being present at the leaf base. Accordingly, a comparison of leaf bases and tips (a spatial distribution) may serve as an orthogonal method of comparing young and old

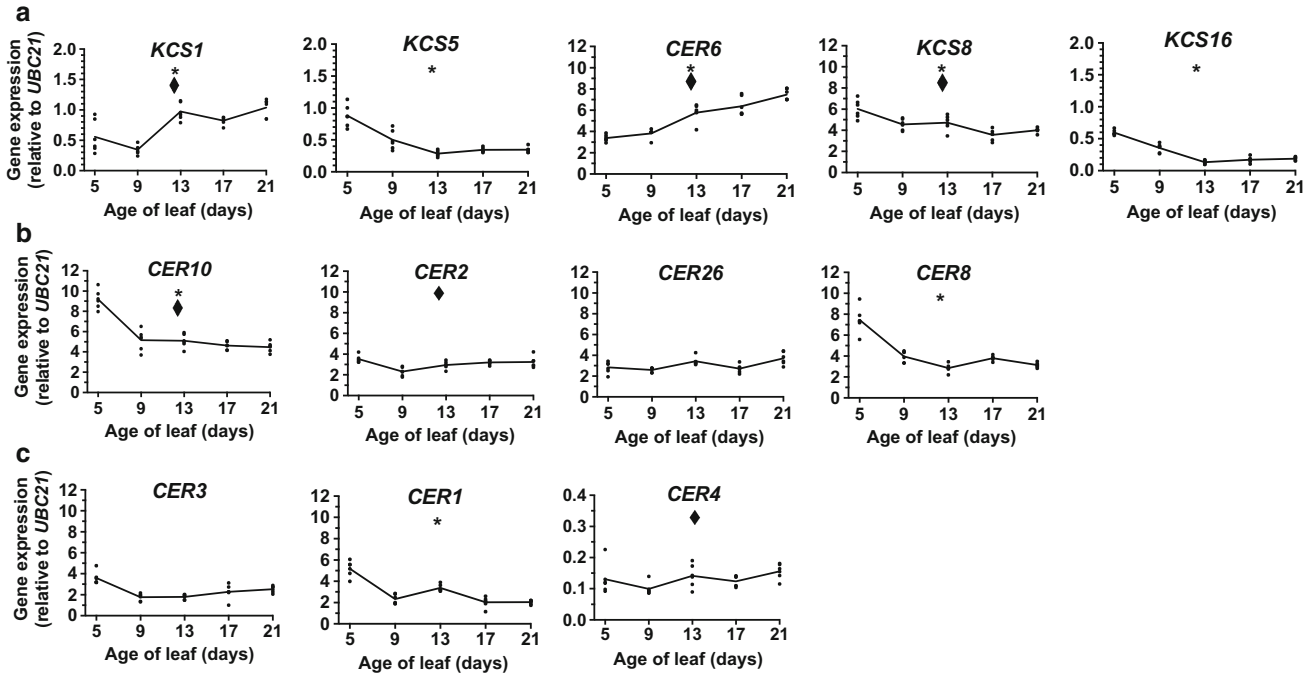

Fig. 7 Expression of wax biosynthesis genes in developing wild-type Arabidopsis eighth leaves. Expression levels were determined using qRT-PCR and normalized against the reference gene *UBC21*. **a** Expression of selected *KCS* genes, encoding the FAE complex enzymes responsible for chain length control during wax precursor elongation. **b** Expression of genes encoding proteins associated with the KCSs during elongation. **c** Expression of genes involved in the conversion of wax precursors into wax compounds. Just as for the chemical data, changes in transcript levels as a function of leaf development between 5 and 21 days of age were analyzed with permutation tests on the robust ordinary least-squares method. Trends found to be significantly different from zero by this test after study-wide adjustment for multiple comparisons were flagged with an *asterisk* (*). Due to apparent inflation of gene expression measurements on day 5, a sensitivity analysis was performed, and trends that were significant upon lightening or omission of day 5 data were flagged with a *diamond* (◆). Details of statistical tests are presented in Appendix S1

leaves (a temporal distribution). Under our growth conditions, the largest difference in cell maturity between tip and base pavement cells was reached at day 13, when tip cells had reached their final size and base cells had only begun to expand, nearly identical to what had been reported for leaf three (Andriankaja et al. 2012).

By both spatial and temporal comparisons, leaves of *gl1* and wild type exhibited decreases in the relative abundance of C_{24}/C_{26} compounds and increases in that of C_{30}/C_{32} compounds or their C_{29} and C_{31} alkane derivatives. A previous analysis of Arabidopsis leaves also found the relative abundance of C_{31} alkane to increase with age, albeit accompanied by a decrease in that of C_{29} alkane (Jenks et al. 1996). Furthermore, an increase in wax compound chain lengths, mostly of alkanes, had been observed on the developing leaves of the monocot *Sorghum bicolor* (Atkin and Hamilton 1950) and diverse dicots including *M. domestica* (Bringe et al. 2006), *S. indicum* (Kim et al. 2009), *C. arabica* (Stocker and Ashton 1975), and *Rhododendron fortunei* (Salasoo 1983). In contrast, leaves of *K. daigremontiana* (van Maarseveen et al. 2009) and several *Triticum* spp. exhibited alkane shortening as they developed (Tulloch 1973; van Maarseveen et al. 2009).

Chain length profiles of wax compounds are established by elongation in FAE complexes, within which the KCS enzymes are known to exert control over product chain length distributions (Fehling and Mukherjee 1991; Millar and Kunst 1997). Consequently, it seems plausible that differential expression of one or more KCS enzymes may lead to the observed shift from C_{24}/C_{26} to C_{30}/C_{32} wax compounds. We found that the expression level of each *KCS* gene was different, as had been reported previously (Joubès et al. 2008; Kim et al. 2013), and that in many cases these expression levels also varied over the course of leaf development. Expression of *KCS5*, *KCS8*, and *KCS16* decreased with age, indicating that these are probably not involved in the increase of C_{30}/C_{32} wax compounds. In contrast, expression of *KCS1* increased with leaf age, thus paralleling the main chain length shift. However, heterologous expression of *KCS1* had yielded C_{20}–C_{26} products (Trenkamp et al. 2004), and the *kcs1* mutant had been found to be affected mainly in the accumulation of C_{26} and C_{28} wax compounds (Todd et al. 1999), together suggesting that this enzyme is likely not involved in the observed chain length shift. In contrast, *CER6* was highly and increasingly expressed throughout leaf development.

This KCS had produced C_{30} and C_{32} compounds when heterologously expressed with *CER2* and *CER26* (Haslam et al. 2012; Pascal et al. 2013; Haslam et al. 2015), and the *cer6* mutant had been found to accumulate C_{26} compounds (Jenks et al. 1995; Fiebig et al. 2000; Hooker et al. 2002). Together with these literature data, our observations now strongly suggest that the turnover of C_{26} acyl-CoA precursors and the resulting accumulation of C_{30}/C_{32} products that characterizes Arabidopsis leaf development are largely controlled by the expression level of *CER6*.

Since CER2 and the CER2-like proteins are also involved in chain elongation by allowing CER6 to produce compounds with 30 or more carbons (Haslam et al. 2012, 2015; Pascal et al. 2013), it seemed plausible that they may also play a role in the developmental chain length shift observed here. However, the expression levels of the *CER2-like* genes did not change during leaf development, making their involvement in the shift unlikely. Their constant expression levels also imply that the abundance of *CER6* transcripts initially limits the production of longer chain lengths. *CER8* showed only a slight decrease in expression levels mainly during early development, making it unlikely that the encoded LACS enzyme probably forming acyl-CoAs from fatty acids (Lu et al. 2009) has a role in driving the chemical changes.

In addition to the chain length shift, our temporal and spatial wax comparisons also revealed a compound class shift from fatty acids to alkanes. This trend is similar to a previous report on Arabidopsis leaf wax development (Jenks et al., 1996), except for the higher overall amounts of fatty acids found here. Many other species exhibit compound class shifts similar to what has been observed for Arabidopsis, including *C. arabica* (Stocker and Ashton 1975), *P. laurocerasus* (Jetter and Schäffer 2001), and *M. domestica* (Bringe et al. 2006), though in some, such as *Sorghum bicolor*, both fatty acids and alkanes continue to accumulate as leaves age (Atkin and Hamilton 1950).

The head group modification pathways generate the different compound classes, and the expression levels of genes encoding respective modifying enzymes are, therefore, prime candidates for instigators of the observed compound class shift. However, the expression levels of *CER3*, *CER1*, and *CER4* suggest that a balance of head-group-modifying enzymes for the alkane- and alcohol-forming pathways is maintained by relatively constant expression of all genes encoding them. Therefore, the drastic change in chemical composition from acids to alkanes cannot be explained by differential expression of the genes coding for head-group-modifying enzymes.

While it is possible that the shift from fatty acids to alkanes is the consequence of the downregulation of a gene responsible for acid formation, no such enzyme activity has been identified. Alternatively, the increase in alkane abundance could arise from the increase in *CER6* expression if the precursors generated by CER6 are channeled preferentially into the alkane pathway instead of being equally available to the alcohol-, alkane-, and acid-forming pathways. Such association between KCS enzymes and head group modification pathways could also explain the selective effect of *kcs1* on the alcohol and acid compound classes (Todd et al. 1999).

Finally, it should be noted that, in addition to the increase in the relative abundance of C_{30}/C_{32}, there was also a significant decrease in C_{34} products (mainly in the form of C_{33} alkane) during development of both *gl1* and wild-type leaves (compare Fig. 3b). This trend might be due to gradually decreasing expression of an unknown KCS with C_{34} product specificity, or to a steady increase in competition between that KCS and the more abundant CER6. The latter explanation would imply that the products of the CER6-containing FAE, C_{30}/C_{32} acyl-CoAs, preferentially serve as substrates for alkane formation (by CER3 and CER1) rather than for further elongation, thus providing further support for substrate channeling from the CER6-containing FAE into the alkane-forming pathway.

Leaf expansion effects on wax coverage

The total wax coverage on mature wild-type leaves was ca. 0.9 μg/cm^2, well within the range of literature values (0.5–1.8 μg/cm^2) for this ecotype (Bourdenx et al. 2011; Bernard et al. 2012; Haslam et al. 2012; Pascal et al. 2013). We found that the glabrous leaves of *gl1* had a roughly constant coverage of ca. 0.6 μg/cm^2 at all stages of development, approximately 65–70 % of the macroscopic coverage of the corresponding wild type, which is consistent with previously reported ratios (Reisberg et al. 2012). It should be noted that the wild-type wax coverages presented here, like those in previous reports, were calculated based on projected, macroscopic leaf surface area, thus ignoring the contribution of trichomes to the true, microscopic surface area.

High trichome densities on young leaves and steady decreases in trichome density during leaf expansion had been reported for many species such as *Bemisia tabaci* and Arabidopsis (Chu et al. 2001; Mauricio 2005; Fabre et al. 2016). Furthermore, a decrease in macroscopic wax coverage with age/expansion was observed on leaves of trichome-bearing species such as Arabidopsis (Jenks et al. 1996), *M. domestica* (Bringe et al. 2006), *S. indicum* (Kim et al. 2009), *H. helix* (Viougeas et al. 1995), and *F. sylvatica* (Gülz et al. 1992), but was not observed on leaves lacking trichomes, such as those of *K. daigremontiana* (van Maarseveen et al. 2009). Overall, these observations indicate that the decrease in macroscopic coverage on developing leaves is probably due to a decrease in trichome

density brought on by pavement cell expansion while no new trichome cells developed.

Due to their complex geometry, the surface area of Arabidopsis leaf trichomes and their contribution to the total leaf surface area are difficult to assess accurately. We counted an average of 75 trichomes on eighth leaves regardless of their age, a number roughly similar to previous reports and well within the range of counts that had been reported for different rosette leaves (Esch et al. 2003). Approximating a trichome as a cylinder (of 50 µm diameter and 150 µm height) topped with three cones (each 20 µm across and 150 µm high; Marks 1997), we estimate the sum surface area of all trichomes on the blade to be 0.03 cm^2. Consequently, trichomes may add ca. 15 and 1 % to the projected surface area of young and mature eighth leaves, respectively. By combining the trichome and pavement cell surfaces, the overall surface area of young and mature leaves must be corrected to 0.23 and 2.83 cm^2, respectively. The wax coverages of wild-type leaves may accordingly be re-calculated, resulting in coverages of ca. 0.9 µg/cm^2 irrespective of age. Thus, wax coverages are roughly constant during growth of both wild-type and *gl1* leaves, as has been observed for growing Arabidopsis stems (Suh et al. 2005), together suggesting that wax production is synchronized with cell expansion.

To maintain constant wax coverage on expanding leaf surfaces, the epidermis must produce wax at a particular rate. According to published expansion rates and coverages for Arabidopsis stem segments (Suh et al. 2005), the rapidly expanding stem tops produced wax at ca. 1.1 µg/day, while the middle of the stem produced 0.15 µg/day. Based on the surface expansion of wild-type eighth leaves (0.16 cm^2/day), we estimate a wax production of ca. 0.15 µg/day between days 5 and 21, or 0.06 µg/cm2 of newly formed surface per day and 0.24 µg per day and fold increase in surface (Table S8). Similar calculations may be performed for specific epidermal cell types by first determining cell-specific wax coverage. Based on their approximated surface area (0.03 cm^2), the difference in the absolute wax amounts on young and mature wild-type leaves (0.05 µg), and the time it takes for a trichome to expand fully (1.5 days), trichome cells should produce wax at a rate of roughly 400 pg day^{-1} $cell^{-1}$ (Table S8). For pavement and guard cells together, this rate is approximately 1.7 pg day^{-1} $cell^{-1}$. Overall, these estimations show that rates of wax production vary considerably between cell types and organs to maintain constant coverage, suggesting that wax production is tightly linked to (cell) surface area expansion rates. The mechanisms controlling this synchrony at the cell- and organ-specific levels are far from clear, and may comprise genetic, biochemical, and/or physiological feedback regulation.

Epidermal cell-type effects on wax composition

Fluctuations in trichome density may not only affect total wax coverage but also wax composition. We found a significant, time-dependent decrease in the relative abundance of C_{35} and C_{37} alkanes and alkenes on wild-type leaves that was not observed on *gl1* leaves (cf. Figs. 3, 4), suggesting that these compounds may differ in their contributions to the total wax loads covering pavement cells and trichomes. This notion can be further investigated by approximating a trichome-specific wax composition by subtracting the wax composition of young (adaxial and abaxial) pavement and guard cells (i.e., the *gl1* wax mixture) from the wax composition of young (adaxial and abaxial) pavement, guard, and trichome cells (i.e., the wild-type wax mixture). As had been reported by others, we did not observe any abaxial trichomes on wild-type leaves, the number of which varies with ecotype, leaf number, and light conditions (Telfer et al. 1997). Thus, this subtractive comparison reflects the adaxial trichome wax composition, which we estimate to consist of *n*-alcohols (ca. 15 % of calculated total trichome wax), alkanes (62 %), and alkenes (ca. 15 %), with each compound class dominated by respective C_{32+} homologs (Fig. S2; Table S9).

To evaluate chain length differences between wax mixtures on trichomes and pavement cells, the calculated trichome wax composition can be compared against the young *gl1* wax composition reported here. The most abundant alkanes in the calculated trichome wax were C_{31} and C_{33} (ca. 42 and 32 % of all alkanes, respectively, Fig. S2), while the relative abundances of these compounds were reversed in the young *gl1* wax mixture (ca. 34 and 41 %). However, the largest compositional differences were observed for C_{35+} alkanes and alkenes, which amounted to ca. 30 % of all the alkanes and alkenes in the trichome wax mixture, but only 10 % of the alkenes and alkanes on young *gl1* eighth leaves. Together, these comparisons strongly suggest that the wax mixture produced by trichome cells differs from that of pavement cells primarily in that it is enriched in C_{35+} alkanes and alkenes.

To identify gene candidates for the production of C_{33}–C_{37} compounds, *KCS*s must again be considered. However, although considerable progress has been made in the characterization of *KCS*s, none has been found that produces compounds longer than C_{34}, even with the aid of CER2-like proteins. The data presented here point to *KCS*s specifically involved in trichome wax elongation. The decrease in trichome density was paralleled by apparent decreases in the expression levels of *KCS5*, *KCS8*, and *KCS16*, genes that had also been found expressed preferentially in trichomes (Marks et al. 2009). It should be noted that, since our gene expression measurements convey the average expression level in all leaf cells, it is possible that

the relative expression level of these genes in trichome cells is underrepresented in the data presented here. Consequently, KCS5, KCS8, and KCS16 may be considered as primary candidates for the production of C_{35+} compounds in trichomes. KCS5 and CER6 share 88 % amino acid identity (Joubès et al. 2008), and the two have similar product profiles even when expressed with CER2-like proteins (Trenkamp et al. 2004; Haslam et al. 2015), suggesting that KCS5, like CER6, only produces up to C_{30}/C_{32} precursors. KCS8 and KCS16 show 74 % amino acid identity, are members of the same *KCS* subclass (Joubès et al. 2008), and have highest transcript abundance in leaves (Kim et al. 2013), though *KCS16* is also highly expressed in siliques (Joubès et al. 2008). Based on the currently available data, both these KCSs remain likely candidates for the production of C_{35+} compounds, particularly in Arabidopsis leaf trichomes. We are currently investigating these genes in more detail.

Finally, it is possible that changes in the relative abundance of guard cells may also contribute to observed coverage and/or compositional shifts, especially since wax biosynthesis gene expression within these cells can differ from that of neighboring pavement cells (Gray et al. 2000). However, guard cells are much smaller than both pavement and trichome cells, there were only half as many guard cells as pavement cells present, and the ratio of guard cells to pavement cells remained constant throughout the period of leaf development studied here (cf. Fig. 1). These observations make it unlikely that guard cells contribute to developmental changes in wax coverage and composition.

Conclusions

In this study, we monitored the development of Arabidopsis leaf surfaces using a combination of morphological, chemical, and gene expression measurements. Developmental shifts in the relative abundances of wax compound classes and chain lengths followed the cell cycle arrest front, and could be attributed mainly to differential expression of *CER6*. Furthermore, the elongation-associated enzymes CER2 and CER26 seem to be present in relatively high abundance early in leaf development, awaiting increase in CER6 transcript/protein availability to produce additional wax compounds of higher chain length. The mechanism by which alkanes become the dominant compound class as the leaf ages is unknown; however, it seems possible that *CER6*-derived wax precursors may have a higher likelihood of entering the alkane pathway than other pathways. Based on these findings, it is interesting to speculate on possible reasons for the synchrony between cell expansion and the shifts in wax composition, and how these may relate to the development of leaf structure and function. Cuticular wax affects the mechanical properties of the cuticle (Tsubaki et al. 2013), and high alkane abundance may be correlated with an effective transpiration barrier and high temperature tolerance (Leide et al. 2007; Ni et al. 2013). Thus, perhaps a fatty acid-rich wax mixture is advantageous early during leaf expansion, and a more alkane-rich wax mixture during late expansion and beyond. Though conjecture, these interpretations represent possible directions for future research.

Author contribution statement LB, DH, and RJ designed the experiments; LB and DH performed the experiments; LB, DH, and RJ analyzed the data; EK designed and performed statistical tests; and LB, DH, EK, and RJ prepared the figures and wrote the manuscript.

Acknowledgments The authors thank Mrs. Yan Cao for skillful technical assistance. Seeds of the trichome-less *gl1* mutant were obtained from the Arabidopsis Biological Resource Center (ABRC). This work has been supported by the Natural Sciences and Engineering Research Council (Canada), the Canada Foundation for Innovation, the British Columbia Knowledge Development Fund, and the Canada Research Chairs Program.

References

Andriankaja M, Dhondt S, De Bodt S, Vanhaeren H, Coppens F, De Milde L, Mühlenbock P, Skirycz A, Gonzalez N, Beemster GTS et al (2012) Exit from proliferation during leaf development in *Arabidopsis thaliana*: a not-so-gradual process. Dev Cell 22:64–78

Atkin DSJ, Hamilton RJ (1950) The changes with age in the epicuticular wax of *Sorghum bicolor*. J Nat Prod 45:697–703

Bazzaz FA, Chiariello NR, Coley PD, Pitelka LF (2016) Allocating resources to reproduction and defense. Bioscience 37:58–67

Benjamini Y, Hochberg Y (1995) Controlling the false discovery rate: a practical and powerful approach to multiple testing. J R Stat Soc Ser B 57:289–300

Bennett RN, Wallsgrove RM (1994) Secondary metabolites in plant defence mechanisms. New Phytol 127:617–633

Bernard A, Domergue F, Pascal S, Jetter R, Renne C, Faure J-D, Haslam RP, Napier JA, Lessire R, Joubès J (2012) Reconstitution of plant alkane biosynthesis in yeast demonstrates that *Arabidopsis* ECERIFERUM1 and ECERIFERUM3 are core components of a very-long-chain alkane synthesis complex. Plant Cell 24:3106–3118

Bourdenx B, Bernard A, Domergue F, Pascal S, Léger A, Roby D, Pervent M, Vile D, Haslam RP, Napier JA et al (2011) Overexpression of Arabidopsis *ECERIFERUM1* promotes wax very-long-chain alkane biosynthesis and influences plant response to biotic and abiotic stresses. Plant Physiol 156:29–45

Bringe K, Schumacher CFA, Schmitz-Eiberger M, Steiner U, Oerke E-C (2006) Ontogenetic variation in chemical and physical characteristics of adaxial apple leaf surfaces. Phytochemistry 67:161–170

Buschhaus C, Jetter R (2012) Composition and physiological function of the wax layers coating Arabidopsis leaves: β-amyrin negatively affects the intracuticular water barrier. Plant Physiol 160:1120–1129

Byrne ME (2005) Networks in leaf development. Curr Opin Plant Biol 8:59–66

Chen X, Wang H, Li J, Huang H, Xu L (2013) Quantitative control of *ASYMMETRIC LEAVES2* expression is critical for leaf axial patterning in *Arabidopsis*. J Exp Bot 64:4895–4905

Chu C-C, Freeman TP, Buckner JS, Henneberry TJ, Nelson DR, Natwick ET (2001) Susceptibility of upland cotton cultivars to *Bemisia tabaci* Biotype B (Homoptera: Aleyrodidae) in relation to leaf age and trichome density. Ann Entomol Soc Am 94:743–749

Coley PD, Bryant JP, Chapin SFI (1985) Resource availability and plant antiherbivore defense. Science 230:895–899

Donnelly PM, Bonetta D, Tsukaya H, Dengler RE, Dengler NG (1999) Cell cycling and cell enlargement in developing leaves of *Arabidopsis*. Dev Biol 215:407–419

Efroni I, Eshed Y, Lifschitz E (2010) Morphogenesis of simple and compound leaves: a critical review. Plant Cell 22:1019–1032

Esch JJ, Chen M, Sanders M, Hillestad M, Ndkium S, Idelkope B, Neizer J, Marks MD (2003) A contradictory *GLABRA3* allele helps define gene interactions controlling trichome development in *Arabidopsis*. Development 130:5885–5894

Fabre G, Mazurek S, Daraspe J, Mucciolo A, Sankar M, Humbel BM, Nawrath C (2016) The ABCG transporter PEC1/ABCG32 is required for the formation of the developing leaf cuticle in Arabidopsis. New Phytol 209:192–201

Fehling E, Mukherjee K (1991) Acyl-CoA elongase from a higher plant (*Lunaria annua*): metabolic intermediates of very-long-chain acyl-CoA products and substrate specificity. Biochem Biophys Acta 1082:239–246

Fiebig A, Mayfield JA, Miley NL, Chau S, Fischer RL, Preuss D (2000) Alterations in *CER6*, a gene identical to *CUT1*, differentially affect long-chain lipid content on the surface of pollen and stems. Plant Cell 12:2001–2008

Fraenkel G (1959) The raison d'etre of secondary plant substances. Science 129:1466–1470

Glover BJ (2000) Differentiation in plant epidermal cells. J Exp Bot 51:497–505

Granier C, Massonnet C, Turc O, Muller B, Chenu K, Tardieu F (2002) Individual leaf development in *Arabidopsis thaliana*: a stable thermal-time-based programme. Ann Bot 89:595–604

Gray JE, Holroyd GH, van der Lee FM, Bahrami AR, Sijmons PC, Woodward FI, Schuch W, Hetherington AM (2000) The HIC signalling pathway links CO_2 perception to stomatal development. Nature 408:713–716

Guimil S, Dunand C (2007) Cell growth and differentiation in *Arabidopsis* epidermal cells. J Exp Bot 58:3829–3840

Gülz P-G, Prasad RBN, Müller E (1992) Surface structures and chemical composition of epicuticular waxes during leaf development of *Fagus sylvatica* L. Z Naturforsch 47c:190–196

Haas K, Schönherr J (1979) Composition of soluble cuticular lipids and water permeability of cuticular membranes from Citrus leaves. Planta 146:399–403

Haslam TM, Mañas Fernández A, Zhao L, Kunst L (2012) Arabidopsis ECERIFERUM2 is a component of the fatty acid elongation machinery required for fatty acid extension to exceptional lengths. Plant Physiol 160:1164–1174

Haslam TM, Haslam R, Thoraval D, Pascal S, Delude C, Domergue F, Fernández AM, Beaudoin F, Napier JA, Kunst L et al (2015) CER2-LIKE proteins have unique biochemical and physiological functions in very-long-chain fatty acid elongation. Plant Physiol 167:682–692

Herms DA, Mattson WJ (2016) The dilemma of plants: to grow or defend. Q Rev Biol 67:283–335

Hooker TS, Millar AA, Kunst L (2002) Significance of the expression of the CER6 condensing enzyme for cuticular wax production in Arabidopsis. Plant Physiol 129:1568–1580

Isaacson T, Kosma DK, Matas AJ, Buda GJ, He Y, Yu B, Pravitasari A, Batteas JD, Stark RE, Jenks MA et al (2009) Cutin deficiency in the tomato fruit cuticle consistently affects resistance to microbial infection and biomechanical properties, but not transpirational water loss. Plant J 60:363–377

Iwakawa H, Iwasaki M, Kojima S, Ueno Y, Soma T, Tanaka H, Semiarti E, Machida Y, Machida C (2007) Expression of the *ASYMMETRIC LEAVES2* gene in the adaxial domain of Arabidopsis leaves represses cell proliferation in this domain and is critical for the development of properly expanded leaves. Plant J 51:173–184

Jakoby MJ, Falkenhan D, Mader MT, Brininstool G, Wischnitzki E, Platz N, Hudson A, Hülskamp M, Larkin J, Schnittger A (2008) Transcriptional profiling of mature Arabidopsis trichomes reveals that *NOECK* encodes the MIXT-like transcriptional regulator MYB106. Plant Physiol 148:1538–1602

Jenks MA, Tuttle HA, Eigenbrode SD, Feldmann KA (1995) Leaf epicuticular waxes of the *eceriferum* mutants in *Arabidopsis*. Plant Physiol 108:369–377

Jenks MA, Tuttle HA, Feldmann KA (1996) Changes in epicuticular waxes on wildtype and *ECERIFERUM* mutants in *Arabidopsis* during development. Phytochemistry 42:29–34

Jetter R, Schäffer S (2001) Chemical composition of the *Prunus laurocerasus* leaf surface. Dynamic changes of the epicuticular wax film during leaf development. Plant Physiol 126:1725–1737

Joubès J, Raffaele S, Bourdenx B, Garcia C, Laroche-Traineau J, Moreau P, Domergue F, Lessire R (2008) The VLCFA elongase gene family in *Arabidopsis thaliana*: phylogenetic analysis, 3D modelling and expression profiling. Plant Mol Biol 67:547–566

Kearns EV, Assmann SM (1993) The guard cell-environment connection. Plant Physiol 102:711–715

Kim M-S, Shim K-B, Park S-H, Kim K-S (2009) Changes in cuticular waxes of developing leaves in sesame (*Sesamum indicum* L.). J Crop Sci Biotechnol 12:161–167

Kim J, Jung JH, Lee SB, Go YS, Kim HJ, Cahoon R, Cahoon EB, Markham JE, Suh MC (2013) *Arabidopsis* 3-ketoacyl-CoA synthase 9 is involved in the synthesis of tetracosanoic acids as precursors of cuticular waxes, suberins, sphingolipids, and phospholipids. Plant Physiol 162:567–580

Lai C, Kunst L, Jetter R (2007) Composition of alkyl esters in the cuticular wax on inflorescence stems of *Arabidopsis thaliana cer* mutants. Plant J 50:189–196

Larkin JC, Brown ML, Schiefelbein J (2003) How do cells know what they want to be when they grow up? Lessons from epidermal patterning in Arabidopsis. Annu Rev Plant Biol 54:403–430

Leide J, Hildebrandt U, Reussing K, Riederer M, Vogg G (2007) The developmental pattern of tomato fruit wax accumulation and its impact on cuticular transpiration barrier properties: effects of a deficiency in a β-ketoacyl-coenzyme A synthase (LeCER6). Plant Physiol 144:1667–1679

Li F, Wu X, Lam P, Bird D, Zheng H, Samuels L, Jetter R, Kunst L (2008) Identification of the wax ester synthase/acyl-coenzyme A: diacylglycerol acyltransferase WSD1 required for stem wax ester biosynthesis in Arabidopsis. Plant Physiol 148:97–107

Lu S, Song T, Kosma DK, Parsons EP, Rowland O, Jenks MA (2009) Arabidopsis *CER8* encodes LONG-CHAIN ACYL-COA SYNTHETASE 1 (LACS1) that has overlapping functions with LACS2 in plant wax and cutin synthesis. Plant J 59:553–564

Marks MD (1997) Molecular genetic analysis of trichome development in Arabidopsis. Annu Rev Plant Physiol Plant Mol Biol 48:137–163

Marks MD, Wenger JP, Gilding E, Jilk R, Dixon RA (2009) Transcriptome analysis of *Arabidopsis* wild-type and *gl3–sst sim* trichomes identifies four additional genes required for trichome development. Mol Plant 2:803–822

Mauricio R (2005) Ontogenetics of QTL: The genetic architecture of trichome density over time in *Arabidopsis thaliana*. Genetica 123:75–85

Millar A, Kunst L (1997) Very-long-chain fatty acid biosynthesis is controlled through the expression and specificity of the condensing enzyme. Plant J 12:121–131

Nath U, Crawford BCW, Carpenter R, Coen E (2003) Genetic control of surface curvature. Science 299:1404–1407

Ni Y, Guo Y-J, Wang J, Xia R-E, Wang X-Q, Ash G, Li J-N (2013) Responses of physiological indexes and leaf epicuticular waxes of *Brassica napus* to *Sclerotinia sclerotiorum* infection. Plant Pathol 63:174–184

Pascal S, Bernard A, Sorel M, Pervent M, Vile D, Haslam RP, Napier JA, Lessire R, Domergue F, Joubès J (2013) The *Arabidopsis cer26* mutant, like the *cer2* mutant, is specifically affected in the very-long-chain fatty acid elongation process. Plant J 73:733–746

Peschel S, Franke R, Schreiber L, Knoche M (2007) Composition of the cuticle of developing sweet cherry fruit. Phytochemistry 68:1017–1025

Pfaffl M (2001) A new mathematical model for relative quantification in real-time RT-PCR. Nucleic Acids Res 29(9):e45

Prasad RBN, Gülz P (1990) Developmental and seasonal variations in the epicuticular waxes of beech leaves (*Fagus sylvatica* L.). Zeitschrift für Naturforsch C 45:805–812

R Core Team (2015) R: a language and environment for statistical computing

Ramsay NA, Glover BJ (2005) MYB-bHLH-WD40 protein complex and the evolution of cellular diversity. Trends Plant Sci 10:63–70

Reisberg EE, Hildebrandt U, Riederer M, Hentschel U (2012) Phyllosphere bacterial communities of trichome-bearing and trichomeless *Arabidopsis thaliana* leaves. Antonie Van Leeuwenhoek 101:551–560

Richardson A, Franke R, Kerstiens G, Jarvis M, Schreiber L, Fricke W (2005) Cuticular wax deposition in growing barley (*Hordeum vulgare*) leaves commences in relation to the point of emergence of epidermal cells from the sheaths of older leaves. Planta 222:472–483

Rowland O, Zheng H, Hepworth SR, Lam P, Jetter R, Kunst L (2006) *CER4* encodes an alcohol-forming fatty acyl-coenzyme A reductase involved in cuticular wax production in Arabidopsis. Plant Physiol 142:866–877

Salasoo I (1983) Effect of leaf age on epicuticular wax alkanes in *Rhododendron*. Phytochemistry 22:461–463

Samuels L, Kunst L, Jetter R (2008) Sealing plant surfaces: cuticular wax formation by epidermal cells. Annu Rev Plant Biol 59:683–707

Schönherr J (1976) Water permeability of isolated cuticular membranes: the effect of cuticular waxes on diffusion of water. Planta 131:159–164

Stocker H, Ashton L (1975) Changes in the composition of coffee wax with development. Phytochemistry 14:1919–1920

Suh MC, Samuels AL, Jetter R, Kunst L, Pollard M, Ohlrogge J, Beisson F (2005) Cuticular lipid composition, surface structure, and gene expression in Arabidopsis stem epidermis. Plant Physiol 139:1649–1665

Sylvester AW, Cande WZ, Freeling M (1990) Division and differentiation during normal and liguleless-1 maize leaf development. Development 110:985–1000

Telfer A, Bollman KM, Poethig RS (1997) Phase change and the regulation of trichome distribution in *Arabidopsis thaliana*. Development 124:645–654

Tian D, Tooker J, Peiffer M, Chung SH, Felton GW (2012) Role of trichomes in defense against herbivores: comparison of herbivore response to woolly and hairless trichome mutants in tomato (*Solanum lycopersicum*). Planta 236:1053–1066

Todd J, Post-Beittenmiller D, Jaworski JG (1999) *KCS1* encodes a fatty acid elongase 3-ketoacyl-CoA synthase affecting wax biosynthesis in *Arabidopsis thaliana*. Plant J 17:119–130

Trenkamp S, Martin W, Tietjen K (2004) Specific and differential inhibition of very-long-chain fatty acid elongases from *Arabidopsis thaliana* by different herbicides. Proc Natl Acad Sci USA 101:11903–11908

Tsubaki S, Sugimura K, Teramoto Y, Yonemori K, Azuma J (2013) Cuticular membrane of *Fuyu persimmon* fruit is strengthened by triterpenoid nano-fillers. PLoS One 8:1–13

Tulloch AP (1973) Composition of leaf surface waxes of *Triticum* species: variation with age and tissue. Phytochemistry 12:2225–2232

van Maarseveen C, Han H, Jetter R (2009) Development of the cuticular wax during growth of *Kalanchoe daigremontiana* (Hamet et Perr. de la Bathie) leaves. Plant Cell Environ 32:73–81

Viougeas MA, Rohr R, Chamel A (1995) Structural changes and permeability of ivy (*Hedera helix* L.) leaf cuticles in relation to leaf development and after selective chemical treatments. New Phytol 130:337–348

Wagner GJ, Wang E, Shepherd RW (2004) New approaches for studying and exploiting an old protuberance, the plant trichome. Ann Bot 93:3–11

Yeats TH, Rose JKC (2013) The formation and function of plant cuticles. Plant Physiol 163:5–20

Zust T, Joseph B, Shimizu KK, Kliebenstein DJ, Turnbull LA (2011) Using knockout mutants to reveal the growth costs of defensive traits. Proc R Soc B Biol Sci 278:2598–2603